ORIGINAL RESEARCH

Effect of sodium lignosulfonate on bonding strength and chemical structure of a lignosulfonate/chitosan-glutaraldehyde medium-density fiberboard adhesive

Chen Liu[1] · Bingnan Yuan[2] · Minghui Guo[2] · Qing Yang[1] · Tat Thang Nguyen[3] · Xiaodi Ji[1]

Abstract

Sodium lignosulfonate/chitosan-glutaraldehyde adhesive (L/C-G) has potential in environment-friendly wood-based panel adhesive applications. However, the effect of sodium lignosulfonate on the bonding strength and chemical structure of L/C-G was not elucidated. Herein, the role of sodium lignosulfonate in L/C-G was studied in detail by characterizing the mechanical properties and water resistance of medium-density fiberboards (MDFs) prepared using L/C-G as adhesives. The functional groups, thermal stability, and crystalline structure of L/C-G with various mass ratios of sodium lignosulfonate to chitosan were also characterized by Fourier transform infrared spectroscopy, thermogravimetric analysis, and X-ray diffraction, respectively. The results show that an appropriate amount of sodium lignosulfonate in L/C-G was beneficial for its bonding strength, and the MDFs with 1:2 mass ratio of sodium lignosulfonate to chitosan showed superior mechanical properties and comparable water resistance with a commercial panel. Besides the reaction between sodium lignosulfonate and chitosan, guaiacyl units, or lateral chain of sodium lignosulfonate might also react with glutaraldehyde and result in C–O–C groups, helpful for the bonding strength of L/C-G.

Keywords Sodium lignosulfonate · Chitosan · Lignosulfonate · MDF · Mechanical property · Water resistance

1 Introduction

With the shrinking of high-quality large-sized timber caused by the depletion of natural forest resources, the medium-density fiberboard (MDF, made from small-sized wood, branches, and forest harvesting slash) industry has expanded rapidly. Traditional adhesives for MDF are usually derived from nonrenewable and depleting fossil resources, and they are made of volatile toxic compounds [1]. The fluctuations in fossil resources and severe environmental pollution caused by the emission of volatile toxic compounds (e.g., formaldehyde) from these adhesives have motivated many researchers and industries to work on the development and utilization of renewable and environment-friendly adhesive sources, such as soy protein [2], wheat protein [3], and starch [4]. However, high costs of these materials and their relatively complex manufacturing processes along with their poor bonding strength and water resistance have limited their industrial applications [5].

Chitosan is a copolymer of *N*-acetyl glucosamine and glucosamine linked by a 1–4 linkage [6], and hence, it contains stacks of amino groups in its framework similar to traditional amino resin adhesives (e.g., urea–formaldehyde resins and melamine resins), and they can endow suitable adherends with outstanding bonding strength [7]. Moreover, chitosan provides water resistance, antibacterial, and antifungal properties for proper adherends [8, 9]. Therefore, chitosan has great potential as multifunctional MDF adhesives. Unlike the raw materials of traditional MDF adhesives, chitosan is derived from an abundant natural polymer, namely, chitin, which is the second most abundant natural

Liu Chen and Bingnan Yuan contributed equally to this work.

✉ Xiaodi Ji
  mingduzhiwang@163.com

1 College of Forestry, Northwest A&F University, Yangling, Shaanxi 712100, People's Republic of China

2 Material Science and Engineering College, Northeast Forestry University, Harbin 150040, People's Republic of China

3 College of Wood Industry and Interior Design, Vietnam National University of Forestry, Xuan Mai, Hanoi 13417, Vietnam

polysaccharide next to cellulose and naturally occurring in crustacean shells, insect exoskeletons, fungal cell walls, microfauna, and plankton [10]. However, unlike traditional MDF adhesives with three-dimensional (3D) networks, the linear structure of chitosan restricts its further applications in MDF industry adhesives made of environment-friendly chitosan.

Crosslinking chitosan with glutaraldehyde can turn chitosan from a linear structure into a 3D network and hence improve its bonding strength [7]. However, the drawback is that the brittleness of adhesive would increase after crosslinking with glutaraldehyde. Moreover, the high cost of chitosan becomes the bottleneck of large-scale application of chitosan in the field of MDF adhesives.

Incorporation of lignosulfonate into glutaraldehyde-crosslinked chitosan might be a promising way to modify this adhesive and enhance its bonding strength. Lignosulfonate is derived from lignin, one of the three main components of wood (the other components are cellulose and hemicellulose) and the second most abundant natural polymer next to cellulose. Lignin plays an essential role in providing rigidity and strength to cell walls as well as acts as an adhesive medium among all the components of cell walls in wood [11]. Moreover, owing to its specific aromatic structure, lignin has attracted much attention as an exceptional substitute for phenol in the production of phenolic adhesives [12]. Hence, lignosulfonate has great potential in the field of MDF adhesives. Nowadays, lignosulfonate is mainly recycled from papermaking industry and is usually directly burnt as fuels, causing a terrible wastage of the natural resource and leading to environmental risk [11]. In fact, lignosulfonate is a water-soluble anionic surfactant containing a large number of functional groups resulting in a unique surfactivity and hence interesting for applications as wood adhesives. Because of these concerns, efficient utilization of lignosulfonate as a green MDF adhesive has attracted much attention of researchers [13].

In our earlier study, a lignosulfonate/chitosan-glutaraldehyde (L/C-G) MDF adhesive was preliminarily prepared by crosslinking lignosulfonate/chitosan using glutaraldehyde, and the effect of glutaraldehyde on its performance was studied [10]. However, the role of lignosulfonate in the adhesive was not elucidated. Therefore, in this study, the effect of lignosulfonate on the bonding strength of this adhesive with various mass ratios of lignosulfonate to chitosan was evaluated in detail based on the characterizations of mechanical and dimensional performance of the corresponding MDFs. The chemical structure of this adhesive was also determined based on the characterizations of functional groups, thermal stability, and crystalline structure of adhesives with the corresponding mass ratios of lignosulfonate to chitosan to further understand the role of lignosulfonate in the synthesis mechanism of this adhesive.

2 Experiment

2.1 Materials

Lignosulfonate (sodium lignosulfonate, CAS No. 8061–51-6) with a sulfonation degree of 1.42 mmol/g was purchased from Wuhan East China Chemical Co. Chitosan (CAS No. 9012–76-4) with a deacetylation degree of more than 95% was supplied by Sun Chemical Technology (Shanghai) Co. Acetic acid (CH_3COOH, CAS No. 64–19-7, AR) was provided by Harbin Kaimeisi Technology Co. Glutaraldehyde ($CHO(CH_2)_3CHO$, 50%, CAS No. 111–30-8, AR) was procured from Tianjin Ruijinte Chemicals Co. Distilled water was prepared in our laboratory. All the chemicals were used as received without further purification. Wood fibers, comprising a mixture of softwood and hardwood fibers from different species, were composed of cellulose (46.70 wt%), hemicelluloses (29.17 wt%), and lignin (22.39 wt%) and supplied by the Greater Khingan Range Hengyou Furniture Co. A commercial MDF with a density of 0.8 g/cm^3 and thickness of 5 mm, which was provided by Oasis Forestry Industry Co. Ltd. and made with urea–formaldehyde resin, was selected as the control.

2.2 Adhesive preparation

The procedure for the synthesis of L/C-G can be described as follows: First, chitosan powder (1 g) and sodium lignosulfonate powder were evenly mixed in a four-necked round-bottom flask. The mass ratios of sodium lignosulfonate and chitosan are shown in Table 1. Then, an appropriate amount of distilled water was added, and the mixture was stirred rapidly at room temperature until the sodium lignosulfonate powder was completely dissolved, and the chitosan powder was evenly dispersed. An acetic acid solution (0.67 g) was then added to the flask. The mixture was stirred at room temperature until chitosan was completely dissolved, and uniform and stable brown viscous sodium lignosulfonate/chitosan (L/C) solution was formed. Next, glutaraldehyde

Table 1 Mass ratio of sodium lignosulfonate and chitosan in L/C-G adhesives

Adhesive code	Mass ratio of sodium lignosulfonate and chitosan
C-G	0
L/C-G 1	1:3
L/C-G 2	1:2
L/C-G 3	1:1
L/C-G 4	2:1
L/C-G 5	3:1

(50 wt%, 1 g) was diluted using distilled water. The L/C served as the primary component of adhesive, and the glutaraldehyde solution served as the crosslinking agent.

2.3 MDF preparation

The procedure for the preparation of MDF can be described as follows: First, the as-made glutaraldehyde solution was added to the L/C solution, and rapid stirring was immediately carried out until the even L/C-G adhesive was formed. Then, the adhesives and wood fibers were added to a high-speed mixer in a mass ratio of sodium lignosulfonate/chitosan and wood fibers of 2.44:100 and agitated at 750 rpm for 5 min. Next, the mixture (moisture content was 60%) of adhesive and wood fibers was removed and manually paved into a 250 mm×250 mm forming box for prepressing to form a slab with a pressure of 1.0 MPa. After that, the box was gently removed, and the slab was placed between the two parallel plates (400 mm×400 mm) of a mechanically controlled oil-heated press for hot pressing at 170 °C for 480s (Fig. S1). A thickness gage with 5 mm was used to ensure that the thickness of MDFs was 5 mm. The as-made MDFs were placed in a room with a constant relative humidity of 40% at room temperature for 2 days, and then the edges of the MDFs were cut off by 30 mm to obtain a dimension of 220 mm×220 mm with a target density of 0.8 ± 0.02 g/cm^3.

2.4 Bonding strength assessment

To evaluate the bonding strength of L/C-G adhesives, the internal bonding strength (IB), modulus of rupture (MOR), modulus of elasticity (MOE), and the 24h thickness swell (24h TS) of MDFs were tested according to the Chinese national standard GB/T 17,657–2013. IB refers to the ratio of the maximum destructive tension perpendicular to the surface of specimen and the area of specimen. It was measured by first adhering the specimen between two steel fixtures and then pulling the two steel fixtures vertically to the specimen surface at a crosshead speed of 0.5 mm/min until the specimen was destroyed. The soft and low-density surfaces of the specimen were sanded to improve the surface smoothness prior to IB tests. MOR refers to the ratio of bending moment to modulus under the maximum load, while MOE refers to the ratio of stress to strain within the elastic limit range of material. MOR and MOE were measured using a three-point bending method at a crosshead speed of 5 mm/min. Twenty-four TS refers to the ratio of thickness increase after immersing in water for 24h at room temperature to the thickness before immersing in water. The MOR and MOE tests were repeated 12 times, while the IB and 24h TS tests were repeated eight times.

2.5 Chemical structure analysis

Fourier transform infrared spectroscopy (FTIR) was used to analyze the functional groups of adhesives using a Nicolet Magna-IR560 E.S.P. FTIR spectrometer and the KBr method in the scanning range of 650–4000 cm^{-1} with 32 times scanning and a resolution of 4 cm^{-1}. Prior to FTIR tests, the adhesive samples were dried at 60 °C and then ground, resulting in adhesive powders. Thermogravimetric analysis (TGA) was conducted to analyze the thermal stability of adhesives using a NET-ZSCH TGA209 thermogravimetric analyzer and operated in the temperature range of 40 to 800 °C at a rate of 10 °C/min under a 30 mL/min nitrogen gas flow. X-ray diffraction (XRD) patterns of the adhesives were obtained using a Rigaku D/max 2200 X-ray diffractometer equipped with a Cu Kα radiation source ($\lambda = 0.15406$ nm) and operated at 40 kV and 30 mA, in the 2θ range of 5–40° and scan rate of 5°/min.

3 Results and discussion

3.1 Effect of sodium lignosulfonate on bonding strength

Figure 1 shows the effect of mass ratio of sodium lignosulfonate to chitosan in L/C-G adhesives on the mechanical properties and dimensional stability of MDFs. With the increase in the mass ratio of sodium lignosulfonate to chitosan in L/C-G adhesives, the change trend of mechanical properties and dimensional stability of MDFs can be divided into two stages. The first stage corresponds to the mass ratio of sodium lignosulfonate to chitosan in the range of 0–1:2. In this stage, with the increase in the mass ratio of sodium lignosulfonate to chitosan, the IB, MOE, and MOR of MDFs increased, while the 24h TS decreased, indicating an improvement in the mechanical properties and dimensional stability of MDF with the increase in the mass ratio of sodium lignosulfonate to chitosan. These results show that an appropriate amount of sodium lignosulfonate in L/C-G adhesives is beneficial to the improvement of mechanical and dimensional stability of MDF.

The second stage corresponds to the mass ratio of sodium lignosulfonate to chitosan in L/C-G adhesives in the range of 1:2 to 3:1. In this stage, with the increase in the mass ratio of sodium lignosulfonate to chitosan, the IB, MOE, and MOR of MDFs did not increase, but decreased unexpectedly, indicating that when the mass ratio of sodium lignosulfonate to chitosan in L/C-G adhesives was more than 1:2, further addition of sodium lignosulfonate would result in a deterioration of the mechanical properties and dimensional stability of MDFs.
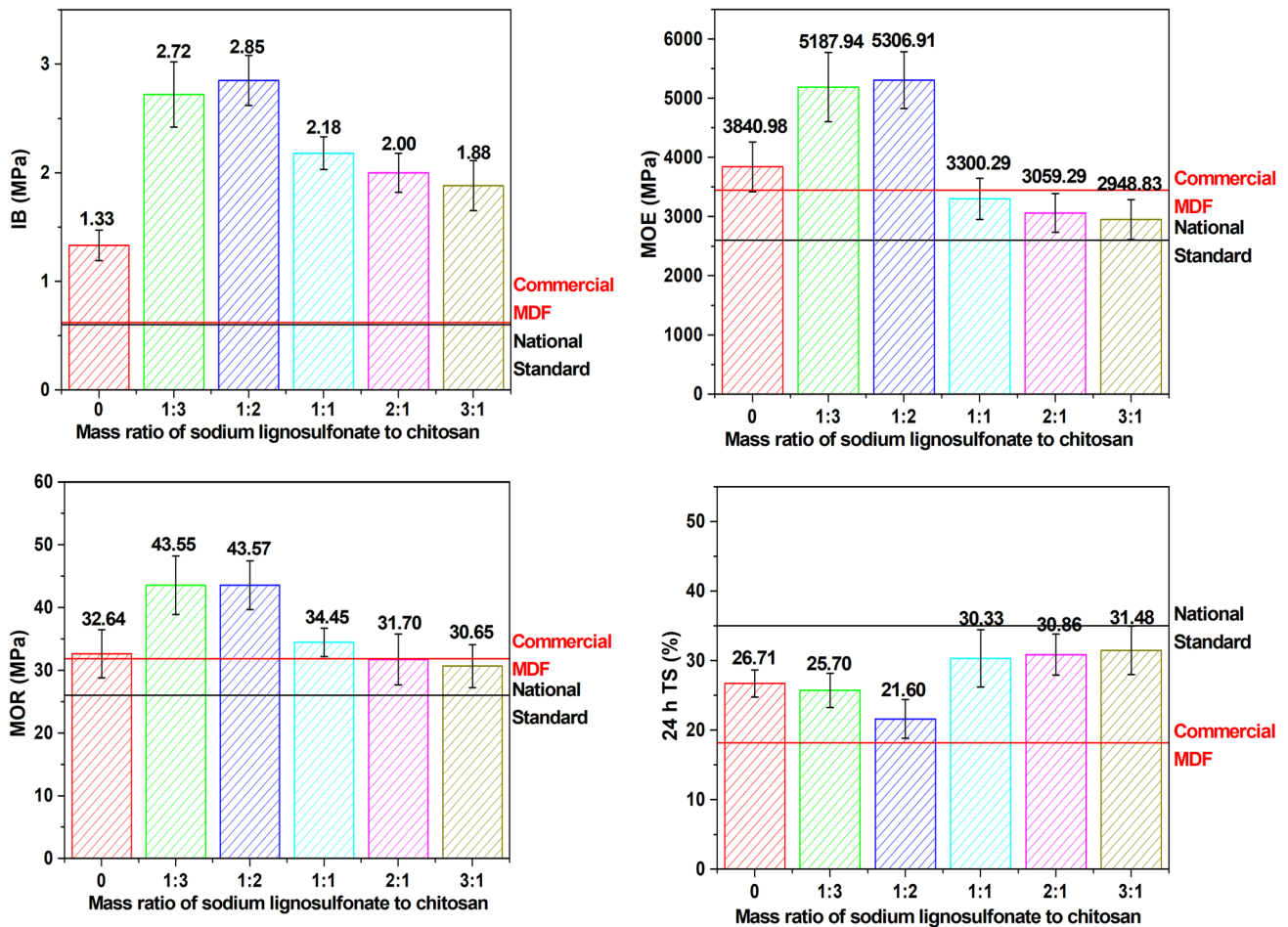
Fig. 1 Mechanical properties and water resistance of MDFs

Notably, in sodium lignosulfonate/chitosan adhesives, the mechanical properties immediately decreased when the mass ratio of sodium lignosulfonate to chitosan was larger than 1:3 [14]. However, for L/C-G, the mechanical properties did not fall immediately when the mass ratio of sodium lignosulfonate to chitosan was in excess of 1:3. The mechanical properties reached the maximum when the mass ratio of sodium lignosulfonate to chitosan increased to 1:2 and then started to decrease with further increase in sodium lignosulfonate content. These results show that the effect of sodium lignosulfonate in L/C-G on the mechanical properties of MDFs was not completely the same as that in L/C. Moreover, for L/C, the 24h TS grew consistently with the increase in the mass ratio of sodium lignosulfonate to chitosan [14]. Similar to L/C-G, the 24h TS first decreased and then increased with the increase in the mass ratio of sodium lignosulfonate to chitosan. Sodium lignosulfonate is hydrophilic. However, an appropriate amount of sodium lignosulfonate in L/C-G was favorable for improving the hydrophobicity of L/C-G, unlike L/C. These results might be related to the role

of sodium lignosulfonate in the synthesis mechanism and chemical structure of L/C-G.

To comprehensively evaluate this MDF, the advantages and disadvantages of mechanical properties and water resistance of this MDF were compared with that in other representative researches (Table 2). The optimal values of IB, MOE, and MOR in this paper were all significantly superior than those in other representative literatures, while the optimal values of 24h TS in this paper did not show distinct advantages than that in other representative literatures.

Overall, the effects of sodium lignosulfonate in L/C-G on the mechanical properties and water resistance of MDFs were basically the same. The IB, MOE, MOR, and 24h TS reached the maximum values when the mass ratio of sodium lignosulfonate to chitosan was 1:2, and the optimal values were 2.85 MPa, 5306.91 MPa, 43.57 MPa, and 21.16%, satisfying the requirements of the Chinese national standard for MDFs (CNS, GB/T 11,718–2009, MDF-GP REG). The mechanical properties of this MDF were much superior than that of commercial MDF and MDFs in other representative literatures, while the water resistance did not show distinct

Table 2 Comparison results of mechanical properties and water resistance of this MDF with that in other representative researches

MDFs	IB (MPa)	MOE (MPa)	MOR (MPa)	24h TS (%)	Reference
In this paper	2.85	5306.91	43.57	21.16	-
With soybean protein adhesive	0.87	2992.11	29.66	28.43	[15]
With ammonium lignosulfonate adhesive	1.71	4157.80	36.96	18.70	[16]
With tannin-modified adhesive	*ca.* 1.4	*ca.* 3200	*ca.* 27.4	*ca.* 7	[17]
Using thermomechanical pulp	*ca.* 0.65	*ca.* 2200	*ca.* 15.5	*ca.* 23	[18]
With crude glycerol and citric acid mixture adhesive	*ca.* 0.9	*ca.* 2450	*ca.* 14.4	*ca.* 10	[19]

advantages, indicating that more work should be conducted to further improve the water resistance of L/C-G in future.

3.2 FTIR analysis

Figures 2 and 3 show the FTIR spectra of sodium lignosulfonate, C-G, and L/C-G with different mass ratios of sodium lignosulfonate to chitosan. For the FTIR spectrum of L/C-G with a mass ratio of sodium lignosulfonate to chitosan of 0, namely, for the FTIR spectrum of C-G, the main peaks were assigned as follows [7]: 3214 cm^{-1} (overlapping of O–H stretching vibration and N–H stretching vibration in original chitosan caused by glutaraldehyde crosslinking), 2931 cm^{-1} and 2866 cm^{-1} (C-H symmetric stretching vibration), 1708 cm^{-1} (C=O stretching vibration), 1652 cm^{-1} (stretching vibration of C=N resulting from the reaction between the amino groups in chitosan and aldehyde groups in glutaraldehyde), 1552 cm^{-1} (overlapping of C-N in amide II band in chitosan and C=C resulting from the aldol reaction of glutaraldehyde), 1255 cm^{-1} (bending vibration of NH in amide III band in chitosan), 1030 cm^{-1} (C–O–C stretching vibrations), and 892 cm^{-1} (characteristic peak of β-1,4-glycosidic bond). For the FTIR spectrum of sodium

lignosulfonate, the characteristic peaks were assigned as follows: 3259 cm^{-1} (-OH stretching vibrations), 2967 cm^{-1} and 2931 cm^{-1} (-CH symmetric stretching vibrations), 1585 cm^{-1} and 1413 cm^{-1} (stretching vibrations of aromatic skeleton), 1119 cm^{-1}, 878 cm^{-1}, and 770 cm^{-1} (bending vibrations of guaiacyl unit), 1046 cm^{-1} (S=O symmetric stretching of the -SO$_3$ groups), and 973 cm^{-1} (out-plane bending vibrations of aromatic skeleton) [14].

Compared with the FTIR spectrum of C-G, a new peak appeared in the FTIR spectra of L/C-G at 2967 cm^{-1} with the gradual increase in the mass ratio of sodium lignosulfonate to chitosan, corresponding to the CH stretching vibration in sodium lignosulfonate. At the same time, the peak at 2931 cm^{-1} corresponds to the increase in CH stretching vibration, and the peak at 2866 cm^{-1} corresponds to the decrease in CH stretching vibration, consistent with the change trend in the FTIR spectra of sodium lignosulfonate/chitosan adhesives [14]. The peak at 1552 cm^{-1} in the FTIR spectrum of C-G corresponds to the overlapping of C-N in amide II band in chitosan and C=C resulting from the aldol reaction of glutaraldehyde [20]. This peak gradually shifted to higher wavenumbers with the increase
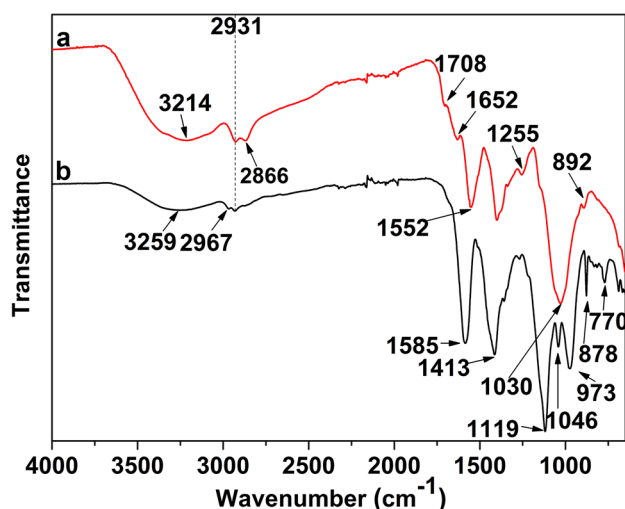

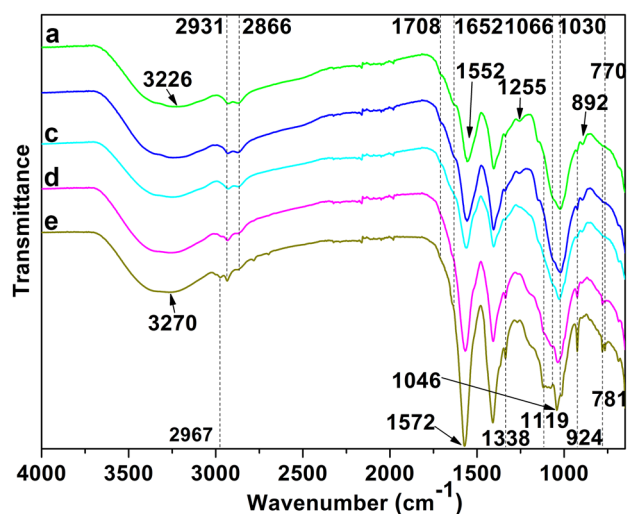**Fig. 2** FTIR spectra of (**a**) C-G and (**b**) sodium lignosulfonate

Fig. 3 FTIR spectra of L/C-G with different mass ratios of sodium lignosulfonate to chitosan: (**a**) 1:3, (**b**) 1:2, (**c**) 1:1, (**d**) 2:1, and (**e**) 3:1

in the mass ratio of sodium lignosulfonate to chitosan in L/C-G and finally moved to 1572 cm^{-1} in the FTIR spectrum of L/C-G 5, because this peak was finally overlapped with the peak of stretching vibration of aromatic ring in sodium lignosulfonate [14].

Figures 2 and 3 show that the intensities and positions of some peaks changed simply owing to the improvement of sodium lignosulfonate content in L/C-G, while the intensities and positions of the other peaks changed owing to the reaction between the growing sodium lignosulfonate and chitosan or glutaraldehyde. The broad peak in the FTIR spectrum of C-G at 3214 cm^{-1} shifted to higher wavenumbers with the increase in the mass ratio of sodium lignosulfonate to chitosan in L/C-G and finally moved to 3270 cm^{-1} in the FTIR spectrum of L/C-G 5. The number of free hydroxyl and amino groups in C-G was more than that of free hydroxyl groups in sodium lignosulfonate, forming more hydrogen bonds in C-G than in sodium lignosulfonate. Hence, the number of hydrogen bonds in L/C-G gradually decreased with the increase in sodium lignosulfonate content; thus, the corresponding peak gradually shifted to higher wavenumbers with the increase in sodium lignosulfonate. The changes in peaks at 1338 cm^{-1}, 924 cm^{-1}, and 781 cm^{-1} correspond to the formation of amide groups and sulfonamide groups between chitosan and sodium lignosulfonate, as described in detail in our previous study [21–25]. The peak in the FTIR spectrum of C-G at 1030 cm^{-1} corresponds to C–O–C stretching vibrations. Unexpectedly, its intensity did not significantly decrease with the increase in the mass ratio of sodium lignosulfonate to chitosan. Besides, a broad band from 1066 to 1119 cm^{-1} gradually formed with the increase in the mass ratio of sodium lignosulfonate to chitosan. This broad band corresponds to the overlapping of bending vibrations in the CH of guaiacyl unit in 1119 cm^{-1} and C–O–C vibrations [26]. Thus, it was inferred that C–O–C linkages

might be formed between glutaraldehyde and sodium lignosulfonate. The peaks at 1119 cm^{-1}, 878 cm^{-1}, and 770 cm^{-1} correspond to the bending vibrations of guaiacyl units. However, the peaks at 1119 cm^{-1} and 770 cm^{-1} did not appear in the FTIR spectra of L/C-G until the mass ratio of sodium lignosulfonate to chitosan was increased to 2:1, while the peak at 878 cm^{-1} disappeared in the FTIR spectra of L/C-G. This indicates that the guaiacyl units might react with glutaraldehyde, and only when sodium lignosulfonate was sufficient, the characteristic peaks correspond to the CH deformation in guaiacyl units. Therefore, it could be assumed that the guaiacyl units of sodium lignosulfonate might react with glutaraldehyde, resulting in the formation of C–O–C linkages.

3.3 Thermal analysis

The thermogravimetric (TG) and derivative TG (DTG) curves of C-G, L-C/G, and sodium lignosulfonate are shown in Fig. 4, and the TG-DTG analysis results are shown in Table 3. Water evaporation occurred below 100 °C, and this weight loss stage is not listed in Table 3.

For sodium lignosulfonate, a weight loss peak was observed at 127.71 °C, corresponding to the breaks of aliphatic hydroxyl groups, carbonyl groups, and C–C bonds in the lateral chains of sodium lignosulfonate [27]. This weight loss peak was not observed in the TG-DTG curves of L/C-G. Notably, this weight loss peak was present in the TG-DTG curves of L/C adhesives [14], indicating that chitosan would not influence the decomposition of lateral chains of sodium lignosulfonate. These results indicate that glutaraldehyde might affect the thermal decomposition of lateral chains of sodium lignosulfonate. Hence, it might indicate that a potential reaction occurred between the lateral chains of sodium lignosulfonate and glutaraldehyde.
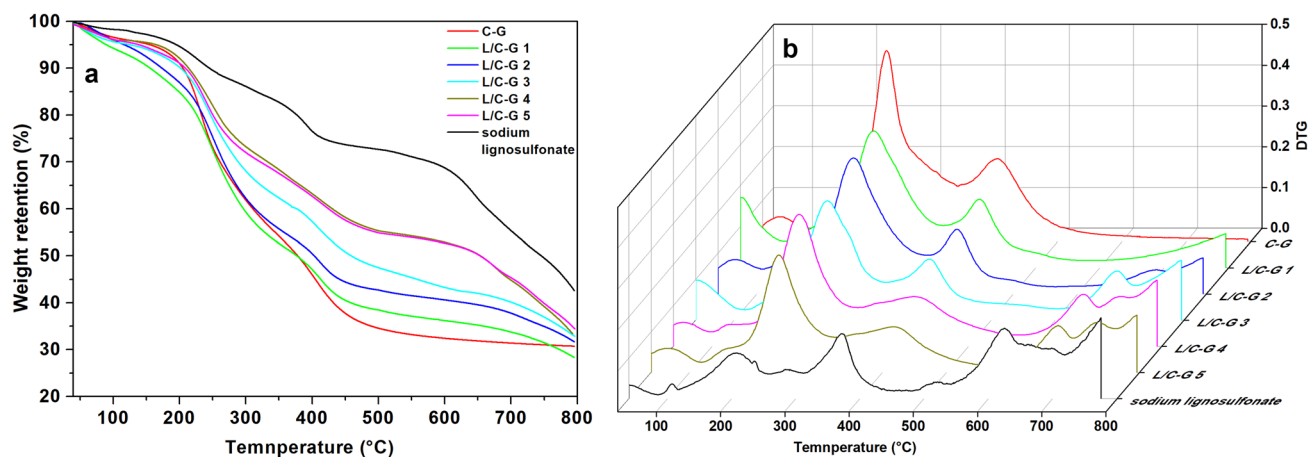

Fig. 4 TG (**a**) and DTG (**b**) curves of sodium lignosulfonate, C/G, and L/C-Gs

Table 3 Results of TG-DTG curves of (a) C-G, L/C-G with different mass ratios of sodium lignosulfonate to chitosan: (b) 1:3, (c) 1:2, (d) 1:1, (e) 2:1, (f) 3:1, and (g) sodium lignosulfonate

Sample	Stage A		Stage B		Stage C		Stage D		Residual amount after 800 °C
	Temperature (°C)	Weight loss (%)	Temperature (°C)	Weight loss (%)	Temperature (°C)	Weight loss (%)	Temperature (°C)	Weight loss (%)	
a			233.07	40.92	405.85	24.35			30.71
b			247.63	39.35	412.22	20.28			28.3
c			250.6	38.05	411.84	17.23	722.07	5.68	31.64
d			245.05	31.77	404.3	16.02	696.18	4.55	32.82
e			235.87	26.01	413.72	15.88	678.48	8.99	34.44
f			238.79	25.42	417.57	13.19	673.7	8.04	33.42
g	127.71	0.7	228.28	8.16	392.01	16.73	645.24	14.51	42.62

The weight loss of sodium lignosulfonate at the temperature range of 230–260 °C corresponds to the thermal decomposition of phenolic compounds (aromatic rings, hydroxyl groups, and alkyl groups). For C-G, this weight loss corresponds to the degradation of hydrogen bonds and polymer chains. The thermal degradation of hydrogen bonds and polymer chains of chitosan occurred at around 286 °C, which shifted to lower temperatures after crosslinking with glutaraldehyde [7]. Therefore, the weight loss peaks observed in the TG-DTG curves of L/C-G between 230 and 260 °C were the overlapping of thermal decomposition of phenolic compounds in sodium lignosulfonate and hydrogen bonds and polymer chains of chitosan. Besides, the potential reaction between glutaraldehyde and sodium lignosulfonate might affect the thermal degradation behaviors of L/C-G between 230 and 260 °C. The weight loss of C-G between 230 and 260 °C was higher than that of sodium lignosulfonate [7, 14]. Hence, the weight loss of L/C-G gradually decreased with the increase in the mass ratio of sodium lignosulfonate to chitosan. Notably, sodium lignosulfonate lost slight weight (8.16% of its total weight) between 230 and 260 °C. In the case of L/C-G, although the weight loss in this temperature range decreased with the increase in sodium lignosulfonate content, the weight loss of L/C-G with a 3:1 mass ratio of sodium lignosulfonate to chitosan only decreased to 25.42%, far higher than 8.16%. As mentioned above, a potential reaction occurred between the lateral chains of sodium lignosulfonate and glutaraldehyde. This reaction might also affect the thermal degradation behavior in this temperature range. Moreover, the potential reaction between guaiacyl units in sodium lignosulfonate and glutaraldehyde might also affect the thermal degradation of phenolic compounds in sodium lignosulfonate.

The weight loss of sodium lignosulfonate between 390 and 420 °C corresponds to the thermal decomposition of sulfonic groups, while that of C-G corresponds to the thermal decomposition of self-polymerized glutaraldehyde formed through aldol condensation [7]. Hence, the weight loss peaks observed in the TG-DTG curves of L/C-G can be attributed to the overlapping of sulfonic groups in sodium lignosulfonate and self-polymerized glutaraldehyde. Besides, the sulfonic groups in sodium lignosulfonate would react with the amino groups in chitosan and form sulfonamide groups, which would also undergo thermal degradation in this temperature range. It was found that the weight loss of C-G was higher than that of sodium lignosulfonate in this temperature range [14], so the weight loss of L/C-G decreased with the increase in the mass ratio of sodium lignosulfonate and chitosan. However, when the mass ratio of sodium lignosulfonate to chitosan in L/C-G increased to 3:1, the weight loss in this temperature range decreased to 13.19%, lower than that of sodium lignosulfonate itself. This phenomenon might also be related to the potential reaction between sodium lignosulfonate and glutaraldehyde.

For temperature higher than 600 °C, no distinct weight loss peak was observed in the TG-DTG curves of C-G and L/C-G with a mass ratio of sodium lignosulfonate to chitosan of 0. With the increase in sodium lignosulfonate content in L/C-G, the weight loss peaks gradually appeared. The positions of these peaks are almost the same as the positions of peaks in the TG-DTG curves of sodium lignosulfonate. For temperatures higher than 800 °C, the residual amount of L/C-G increased with the increase in sodium lignosulfonate content, indicating that the addition of sodium lignosulfonate was beneficial to thermal stability when the temperature was higher than 800 °C.

3.4 XRD analysis

The XRD patterns of sodium lignosulfonate, C-G, and L/C-G are shown in Fig. 5. Seven major peaks appeared at 23.1°, 25.9°, 27.2°, 28.2°, 31.5°, 32.5°, and 33.6°, as shown in the XRD pattern of sodium lignosulfonate. The peak at 31.5° was especially sharp [14]. C-G showed a major peak at about 20°. After crosslinking with glutaraldehyde, the ordered linear structure of chitosan would turn
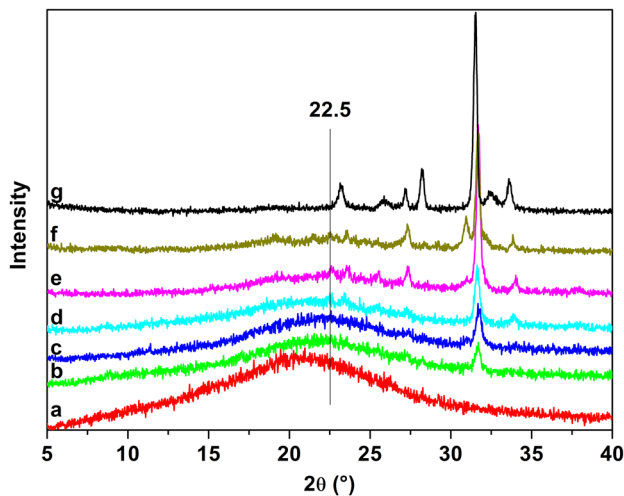
Fig. 5 FTIR spectra of (**a**) C-G, L/C-G with different mass ratios of sodium lignosulfonate to chitosan: (**b**) 1:3, (**c**) 1:2, (**d**) 1:1, (**e**) 2:1, and (**f**) 3:1, and (**g**) sodium lignosulfonate

into an amorphous 3D structure, resulting in an amorphous broad peak at about 20° [7].

In the case of L/C-G, the broad peak at about 20° gradually shifted to higher degrees with the increase in sodium lignosulfonate content and finally shifted to 22.5° at a mass ratio of sodium lignosulfonate to chitosan of 3:1. Meanwhile, this peak gradually narrowed. Besides, a weak sharp peak gradually appeared at 22.5° in the XRD patterns of L/C-G with the increase in sodium lignosulfonate content, which was not observed in the XRD patterns of sodium lignosulfonate, L/C [14], and C-G [7], indicating the potential reaction between guaiacyl units or lateral chains of sodium lignosulfonate and glutaraldehyde. Furthermore, a sharp peak at 30.5° gradually appeared in the TG-DTG curves of L/C-G when the mass ratio of sodium lignosulfonate to chitosan was higher than 2:1, which also appeared in the XRD patterns of L/C [14], but it was not observed in the XRD patterns of sodium lignosulfonate and C-G [7]. This phenomenon is similar to the changes at 1338 cm^{-1}, 924 cm^{-1}, and 781 cm^{-1} in the FTIR spectra of L/C-G. Therefore, these changes also confirm the reaction between chitosan and sodium lignosulfonate, leading to the formation of sulfonamide groups.

From the analysis results of FTIR spectra, TG-DTG curves, XRD patterns, and previously published data, the role of sodium lignosulfonate in the synthesis mechanism and chemical structure of L/C-G was roughly elucidated. Besides the reaction between sodium lignosulfonate and chitosan [14], and chitosan and glutaraldehyde [7], a potential reaction between the lateral chains and guaiacyl units of sodium lignosulfonate and glutaraldehyde might also occur in L/C-G, leading to the formation of C–O–C linkages and benefitting the mechanical properties and water resistance of MDFs.

4 Conclusions

The role of sodium lignosulfonate in the bonding performance and synthesis of L/C-G was analyzed in detail. An appropriate amount of sodium lignosulfonate in L/C-G is conducive to the mechanical properties and water resistance of the corresponding MDFs. The optimal mass ratio of sodium lignosulfonate to chitosan in L/C-G is 1:2, and the corresponding IB, MOE, MOR, and 24h TS values of MDFs are 2.85 MPa, 5306.91 MPa, 43.57 MPa, and 21.16%, respectively, satisfying the requirements of the Chinese national standard for MDFs (CNS, GB/T 11,718–2009, MDF-GP REG). The mechanical properties were also much superior than those of commercial MDFs and MDFs in other representative literatures. Besides the reaction between sodium lignosulfonate and chitosan, sodium lignosulfonate also reacted with glutaraldehyde and thus improved the mechanical properties and water resistance of MDFs. Further research will focus on the elucidation of reaction between glutaraldehyde and sodium lignosulfonate and improvement on MDF water resistance.

Declarations

Conflict of interest The authors declare no competing interests.

References

1. Jiang W, Kumar A, Adamopoulos S (2018) Liquefaction of lignocellulosic materials and its applications in wood adhesives-a review. Ind Crop Prod 124:325–342. https://doi.org/10.1016/j.indcrop.2018.07.053

2. Pradyawong S, Li J, He Z, Sun XS, Wang D, Cheng HN, Klasson KT (2018) Blending cottonseed meal products with different protein contents for cost-effective wood adhesive performances. Ind Crop Prod 126:31–37. https://doi.org/10.1016/j.indcrop.2018.09.052

3. Nordqvist P, Johansson E, Khabbaz F, Malmström E (2013) Characterization of hydrolyzed or heat treated wheat gluten by SE-HPLC and ^{13}C NMR: correlation with wood bonding performance. Ind Crop Prod 51:51–61. https://doi.org/10.1016/j.indcrop.2013.08.057

4. Xing J, Li T, Yu Y, Chen C, Chang J (2018) Development and characterization of a new bio-adhesive for wood using cassava starch and bio-oil. Int J Adhes Adhes 87:91–97. https://doi.org/10.1016/j.ijadhadh.2018.09.005

5. Despres A, Pizzi A, Vu C, Pasch H (2008) Formaldehyde-free aminoresin wood adhesives based on dimethoxyethanal. J Appl Polym Sci 110:3908–3916. https://doi.org/10.1002/app.28936

6. Chen G, Dong S, Zhao S, Li S, Chen Y (2019) Improving functional properties of zein film via compositing with chitosan and cold plasma treatment. Ind Crop Prod 129:318–326. https://doi.org/10.1016/j.indcrop.2018.11.072

7. Ji X, Li B, Yuan B, Guo M (2017) Preparation and characterizations of a chitosan-based medium-density fiberboard adhesive with high bonding strength and water resistance. Carbohydr Polym 176:273–280. https://doi.org/10.1016/j.carbpol.2017.08.100

8. Zhang C, Wang Z, Li Y, Yang Y, Ju X, He R (2019) The preparation and physiochemical characterization of rapeseed protein hydrolysate-chitosan composite films. Food Chem 272:694–701. https://doi.org/10.1016/j.foodchem.2018.08.097

9. Ji X, Guo M (2018) Preparation and properties of a chitosan-lignin wood adhesive. Int J Adhes Adhes 82:8–13. https://doi.org/10.1016/j.ijadhadh.2017.12.005

10. Ji X, Dong Y, Yuan B, Li B, Guo M (2018) Influence of glutaraldehyde on the performance of a lignosulfonate/chitosan-based medium density fiberboard adhesive. J Appl Polym Sci 135:45870. https://doi.org/10.1002/app.45870

11. Kai D, Tan MJ, Chee PL, Chua YK, Yap YL, Loh XJ (2016) Towards lignin-based functional materials in a sustainable world. Green Chem 18:1175–1200. https://doi.org/10.1039/C5GC02616D

12. Kalami S, Chen N, Borazjani H, Nejad M (2018) Comparative analysis of different lignins as phenol replacement in phenolic adhesive formulations. Ind Crop Prod 125:520–528. https://doi.org/10.1016/j.indcrop.2018.09.037

13. Gao S, Cheng Z, Zhou X, Liu Y, Chen R, Wang J, Wang C, Chu F, Xu F, Zhang D (2020) Unexpected role of amphiphilic lignosulfonate to improve the storage stability of urea formaldehyde resin and its application as adhesives. Int J Biol Macromol 161:755–762. https://doi.org/10.1016/j.ijbiomac.2020.06.135

14. Ji XD, Guo MH, Zhu L, Du W, Wang HB (2020) Synthesis mechanism of an environment-friendly sodium lignosulfonate/chitosan medium-density fiberboard adhesive and response of bonding performance to synthesis mechanism. Materials 13:5697. https://doi.org/10.3390/ma13245697

15. Li X, Li Y, Zhong Z, Wang D, Ratto JA, Sheng K, Sun XS (2009) Mechanical and water soaking properties of medium density fiberboard with wood fiber and soybean protein adhesive. Bioresour Technol 100:3556–3562. https://doi.org/10.1016/j.biortech.2009.02.048

16. Hu J-p, Guo M-h (2015) Influence of ammonium lignosulfonate on the mechanical and dimensional properties of wood fiber biocomposites reinforced with polylactic acid. Ind Crop Prod 78:48–57. https://doi.org/10.1016/j.indcrop.2015.09.075

17. Lopez-Suevos F, Riedl B (2003) Effects of *Pinus pinaster* bark extracts content on the cure properties of tannin-modified adhesives

and on bonding of exterior grade MDF. J Adhes Sci Technol 17:1507–1522. https://doi.org/10.1163/156856103769207374

18. Li X, Wu Y, Cai Z, Winandy JE (2013) Primary properties of MDF using thermomechanical pulp made from oxalic acid pretreated rice straw particles. Ind Crop Prod 41:414–418. https://doi.org/10.1016/j.indcrop.2012.04.039

19. Segovia F, Blanchet P, Essoua GGE (2021) Potential of the crude glycerol and citric acid mixture as a binder in medium-density fiberboard manufacturing. Euro J Wood Wood Prod 79:1141–1151. https://doi.org/10.1007/s00107-021-01719-w

20. Bui TH, Lee W, Jeon S-B, Kim K-W, Lee Y (2020) Enhanced Gold(III) adsorption using glutaraldehyde-crosslinked chitosan beads: effect of crosslinking degree on adsorption selectivity, capacity, and mechanism. Sep Purif Technol 248:116989. https://doi.org/10.1016/j.seppur.2020.116989

21. Nawaz A, Li E, Irshad S, Hhm H, Liu J, Shahbaz HM, Ahmed W, Regenstein JM (2020) Improved effect of autoclave processing on size reduction chemical structure nutritional mechanical and in vitro digestibility properties of fish bone powder. Adv Powder Technol 31:2513–2520. https://doi.org/10.1016/j.apt.2020.04.015

22. Sarojini K, Krishnan H, Kanakam CC, Muthu S (2013) Synthesis, structural, spectroscopic studies NBO analysis NLO and HOMO–LUMO of 4-methyl-N-(3-nitrophenyl)benzene sulfonamide with experimental and theoretical approaches. Spectrochim Acta A 108:159–170. https://doi.org/10.1016/j.saa.2013.01.060

23. Kaushal AM, Chakraborti AK, Bansal AK (2008) FTIR studies on differential intermolecular association in crystalline and amorphous states of structurally related non-steroidal anti-inflammatory drugs. Mol Pharmaceut 5:937–945. https://doi.org/10.1021/mp800098d

24. Álvarez RMS, Cutín EH, Mack H-G, Romano RM, Della Védova CO (1997) Vibrational spectra of trifluoromethanesulfonyl isocyanate, CF$_3$SO$_2$NCO. J Raman Spectrosc 28:277–281

25. Sanden KW, Kohler A, Afseth NK, Böcker U, Rønning SB, Liland KH, Pedersen ME (2019) The use of Fourier-transform infrared spectroscopy to characterize connective tissue components in skeletal muscle of Atlantic cod (*Gadus morhua L*). J Biophotonics 12:e201800436. https://doi.org/10.1002/jbio.201800436

26. Shi R, Li B (2016) Synthesis and characterization of cross-linked starch/lignin film. Starch - Stärke 68:1224–1232. https://doi.org/10.1002/star.201500331

27. Li B, Lv W, Zhang Q, Wang T, Ma L (2014) Pyrolysis and catalytic pyrolysis of industrial lignins by TG-FTIR: Kinetics and products. J Anal Appl Pyrol 108:295–300. https://doi.org/10.1016/j.jaap.2014.04.002